

Timing noise, glitches and the braking index of PSR B0540–69[★]

G. Cusumano¹, E. Massaro^{2,3}, and T. Mineo¹

¹ Istituto di Astrofisica Spaziale e Fisica Cosmica – Sezione di Palermo, CNR, via Ugo La Malfa 153, 90146 Palermo, Italy

² Dipartimento di Fisica, Università La Sapienza, Piazzale A. Moro 2, 00185 Roma, Italy

³ Istituto di Astrofisica Spaziale e Fisica Cosmica – Sezione di Roma, CNR, Via del Fosso del Cavaliere, 00100 Roma, Italy

Received 28 May 2002 / Accepted 9 January 2003

Abstract. We report a pulse-time history of PSR B0540–69 based on the analysis of an extended data set including ASCA, BeppoSAX and RXTE observations spanning a time interval of about 8 years. This interval includes also the epoch of the glitch episode reported by Zhang et al. (2001). Our analysis shows the presence of relevant timing noise and does not give clear evidence of the glitch occurrence. We performed an accurate evaluation of the main timing parameters, ν , $\dot{\nu}$ and $\ddot{\nu}$ and derived a mean braking index of $n = 2.125 \pm 0.001$ quite different from the lower value found by Zhang et al. (2001), but in rather good agreement with several other values reported in the literature.

Key words. stars: pulsars: general – stars: pulsars: individual: PSR B0540–69 – X-rays: stars

1. Introduction

PSR B0540–69 was discovered in the soft X-rays by Seward et al. (1984) in a field of the Large Magellanic Cloud observed with the Einstein Observatory. Pulsations at optical frequencies were soon detected by Middleditch & Pennypacker (1985) with a mean pulsed magnitude of 22.5. In the radio band PSR B0540–69 is a quite faint source and pulsed signals were first observed only in 1989–1990 (Manchester et al. 1993).

PSR B0540–69 is one of the youngest rotation powered pulsars. It has a period of about 50 ms and a large period derivative of $4.79 \times 10^{-13} \text{ s s}^{-1}$, comparable to that of the Crab pulsar, and a spin down age of about 1500 years. The pulse shape, at X and optical wavelengths, is broad and almost sinusoidal. Several estimates of the braking index n have been reported in the literature (see Boyd et al. 1995 for a compilation of older results) ranging from 2.01 ± 0.02 (Manchester & Peterson 1989; Nagase et al. 1990) to 2.74 ± 0.10 (Ögelman & Hasinger 1990). Deeter et al. (1998) analyzed an extended set of GINGA observations and found a braking index of 2.08 ± 0.02 . This result was substantially confirmed by Mineo et al. (1999), who combining a BeppoSAX frequency measurement with earlier ASCA results derived a value of 2.10 ± 0.1 , and by Kaaret et al. (2001) also using Chandra observations. A recent analysis of all ASCA pointed observations gave a braking index of 2.10 (Hirayama et al. 2002). A glitch in the timing

history of PSR B0540–69, the only one reported up to now for this young Crab-like pulsar, has been recently pointed out by Zhang et al. (2001). These authors based their analysis on a collection of RXTE observations, spanning 1.2 years. The approximate epoch of the glitch, according to their estimates, occurred on MJD 51325 ± 45 and the change in frequency and its first derivative were $\Delta\nu/\nu = (1.90 \pm 0.04) \times 10^{-9}$ and $\Delta\dot{\nu}/\dot{\nu} = (8.5 \pm 0.07) \times 10^{-5}$, respectively. Zhang et al. (2001) measured also the braking index after the glitch which resulted equal to 1.81 ± 0.07 , significantly lower than the values reported from other analyses.

In this paper we present an exhaustive timing analysis of PSR B0540–69 performed on RXTE data set spanning about 5 years. In particular, we extend the set of RXTE observations used by Zhang et al. (2001), adding more observations for a total time interval of about 3 years before and 2 years after the epoch of the glitch episode claimed by these authors. Moreover, to further increase the time interval data set, public ASCA and BeppoSAX observations are also included in the analysis extending the length up to about 8 years.

2. Observation and data reduction

The RXTE observations considered in the present paper were performed between March 8, 1996 and March 14, 2001. We used only data obtained with the PCA (Jahoda et al. 1996) accumulated in “Good Xenon” telemetry mode, time-tagged with a $1 \mu\text{s}$ accuracy with respect to the spacecraft clock, which is maintained to the UTC better than $100 \mu\text{s}$. The pulsar position inside the instrument Field of View (FoV) is different in the various pointings and ranges between 0 and 25 arcmin

Send offprint requests to: G. Cusumano,
e-mail: giancarlo.cusumano@pa.iasf.cnr.it

[★] Table A1 is only available in electronic form at the CDS via anonymous ftp to cdsarc.u-strasbg.fr (130.79.128.5) or via <http://cdsweb.u-strasbg.fr/cgi-bin/qcat?J/A+A/402/647>

far from the centre. Following Zhang et al. (2001) we considered only events with pulse-height channels between 5 and 50, corresponding to the 2–18 keV energy interval. Furthermore, we verified that the selection of all PCA detector layers, instead of those from the top layer only, increased significantly the S/N ratio of the pulsation and adopted this choice for all the observations.

PSR B0540–69 was observed by ASCA (Tanaka et al. 1994) 14 times between 1993–06–13 and 1999–11–03. Only data from GIS (Ohashi et al. 1996; Makishima et al. 1996) were used in our analysis. The pulsar position inside the FoV ranges between 0 and 22 arcmin off-axis. The Narrow Field Instruments (NFIs) onboard BeppoSAX (Boella et al. 1997a) observed PSR B0540–69 five times between 1996–10–26 and 2000–02–19. We considered only data from MECS (Boella et al. 1996) because they are in the same energy range used for the analysis of the other two satellites. The position of the source inside the instrument FoV lies between 0 and 17 arcmin. Data from both imaging instruments (GIS and MECS) were extracted from regions centered at the source position and the shapes and sizes of these regions were optimized for each observation, depending upon the different off-axis locations, to achieve the highest S/N ratio. The log of all these observations is given in Table A1 (see Appendix).

3. Timing analysis and pulse profile

3.1. Frequencies and derivatives evaluation

The UTC arrival times of all selected events were first converted to the Solar System Barycentre using the (J2000) pulsar position $\alpha = 5^{\text{h}}40^{\text{m}}10^{\text{s}}.95$ and $\delta = -69^{\circ}19'55''.1$ (Caraveo et al. 1992) and the JPL2000 ephemeris (DE200; Standish 1982). For each observation we searched the pulsed frequency ν using the folding technique in a range centered at the values computed by means of the pulsar ephemeris reported by Deeter et al. (1999). The central time of each observation was chosen as the reference epoch and the corresponding frequency was estimated by fitting the χ^2 peak with a Gaussian profile. Both these data are listed in Table A1 (Cols. 2 and 7, respectively). Frequency errors at 1σ level were computed with two different methods. The first evaluation was performed computing the frequency interval corresponding to a unit decrement with respect to the maximum in the χ^2 curve ($err = \nu(\chi_{\text{max}}^2) - \nu(\chi_{\text{max}}^2 - 1)$). In the second method we produced a template profile folding the longest RXTE observation (rows 33+34 in Table A1) with its best frequency (see Fig. 1). The zero phase was taken at the centre of the peak. Then, we compared the folded profiles of other pointings with an accurate analytical model of the template changing the frequency within the searching range and computed the relative χ^2 values. For a correct comparison we subtracted the off-pulse levels and normalized the total pulsed counts. The frequency uncertainties were then set equal to the frequency interval corresponding to an increase of the χ^2 by a unit with respect to the minimum in the curve ($err = \nu(\chi_{\text{min}}^2 + 1) - \nu(\chi_{\text{min}}^2)$). No significant difference was found between the error estimates obtained with the two methods; we then considered as proper statistical uncertainties of the

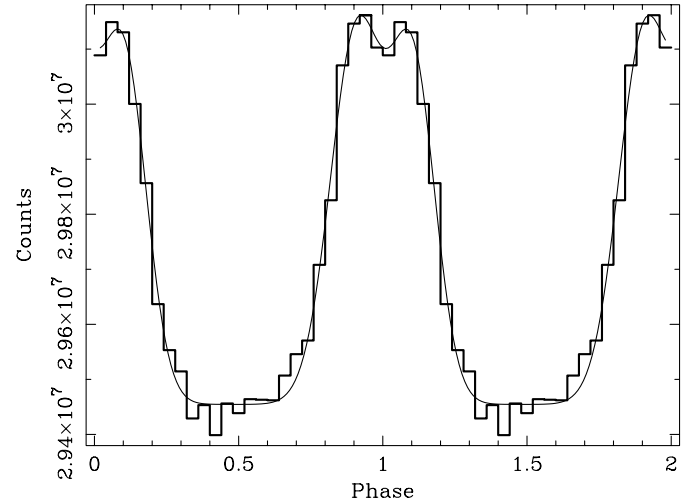


Fig. 1. The (2–18 keV) pulse profile of PSR B0540–69 in 25 phase bins. The analytical model used as template for the timing analysis is also shown.

pulsar frequencies those computed with the first one (Col. 8). All errors, thereafter, refer to one standard deviation. The times of arrival (TOA), referred to the peak centre, were also determined for all RXTE observations by cross-correlating the folded profiles with the analytical model of the template. The resulting phase offset was added to the central time of the observation. Errors on TOAs were assumed equal to the statistical uncertainties of the peak centre derived from a best fit of the pulse profile. TOA and errors are reported in Table A1 (Cols. 5 and 6).

A first estimate of the frequency derivatives was obtained by the best fit of the frequency history listed in Table A1 with the second-degree polynomial:

$$\nu(t) = \nu_0 + \dot{\nu}_0(t - t_0) + \frac{1}{2}\ddot{\nu}_0(t - t_0)^2. \quad (1)$$

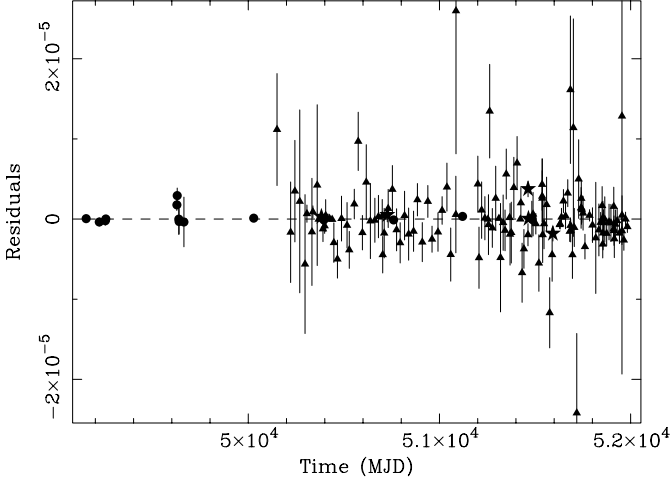
This procedure was first applied separately to the two ASCA+BeppoSAX and RXTE frequency sets and the resulting parameters' values were found in good agreement within their uncertainties. We then evaluated the ephemeris for the whole set of data (RXTE+ASCA+BeppoSAX); a summary of these results is given in Table 1. For easy comparison, the same reference epoch (t_0) was taken, in all the fittings, equal to MJD 50372.5481748585. Figure 2 shows the residuals obtained fitting the entire frequency set with Eq. (1): the number of frequency values in excess of 2 standard deviations is about 6% of the total, confirming the right evaluation of the frequency errors.

3.2. Pulse phase analysis

The precision of the timing parameters can be enhanced by maintaining a pulse coherence over the entire time interval covered by the observations. This analysis was performed only on the RXTE data. The BeppoSAX timing, in fact, does not maintain the indispensable accuracy of the UTC, fundamental to apply a coherent phase analysis. The ASCA observations are rather sparse and the systematics in the absolute time

Table 1. Ephemerides of PSR B0540–69 obtained from a second-degree polynomial fit of the frequency data sets reported in Table A1. 1σ error is given in parentheses for the corresponding last significant digits.

| Data Set | t_0 (MJD) | ν (Hz) | $\dot{\nu}$ ($\times 10^{-10}$ Hz s $^{-1}$) | $\ddot{\nu}$ ($\times 10^{-21}$ Hz s $^{-2}$) |
|--------------------|------------------|----------------|---|--|
| ASCA+BeppoSAX | 50372.5481748585 | 19.81583115(7) | -1.880724(7) | 3.74(2) |
| RXTE | 50372.5481748585 | 19.8158314(1) | -1.8808(1) | 3.73(20) |
| ASCA+BeppoSAX+RXTE | 50372.5481748585 | 19.81583119(4) | -1.880727(8) | 3.717(7) |

**Fig. 2.** Residuals of the best fit of the frequencies obtained by the folding technique with the polynomial formula of Eq. (1). Triangles represents RXTE data, circle ASCA data and stars BeppoSAX data.

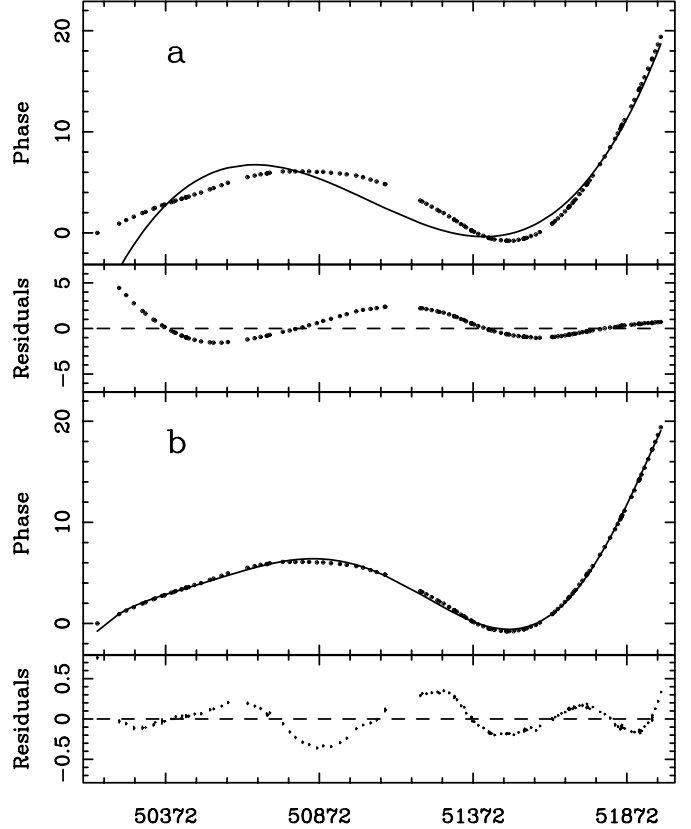
assignment (Hirayama et al. 1996) make more complicated the proper phase cycle correction.

The arrival times in each event for the RXTE observations were folded by using the values of ν_0 , $\dot{\nu}_0$, $\ddot{\nu}_0$ reported in Table 1 (line 3). Phase shifts of the pulse profiles, expected because of the ephemeris accuracy, were computed for all observations by a cross-correlation with the analytical model of the template (Fig. 1). Phase errors were taken equal to the TOA uncertainties multiplied by the corresponding frequencies. Throughout this paper phases are measured in cycle units. The resulting values of the phase shifts, corrected for the presence of recycles, are shown in Fig. 3 as a function of the observation epoch.

The large phase variations, of the order of several cycles in a few hundred days, indicate that input ephemerides of Table 1 are not the best ones and that it is possible to improve them. The corrections, in absence of frequency irregularities, can be obtained by fitting the phase lags by the simple third-degree spin-down model:

$$\Delta\phi(t) = \Delta\nu_0(t - t_0) + \frac{1}{2}\Delta\dot{\nu}_0(t - t_0)^2 + \frac{1}{6}\Delta\ddot{\nu}_0(t - t_0)^3, \quad (2)$$

where $\Delta\phi(t)$ is the measured phase difference at time t , t_0 is the reference epoch and $\Delta\nu_0$, $\Delta\dot{\nu}_0$, $\Delta\ddot{\nu}_0$ are the ephemeris corrections for the frequency, first and second derivatives, respectively. We found that this equation fails to describe the entire set of phase data showing very large systematic deviations (panel a of Fig. 3). Such deviations indicate the presence of a timing

**Fig. 3.** Phase of the pulsed signal, after a careful reconstruction of the phase recycles for the entire set of the RXTE observations, vs observing time. Phase is in cycle units. Panel a) shows the fit with a third order polynomial and panel b) shows the fit with a sixth order polynomial. Data and fitting models are shown in the top, residuals in the bottom.

noise characteristic of several other pulsars (Arzoumanian et al. 1994; Lyne 1999). We tried also to correct the phases by fitting higher order polynomials, up to the sixth degree. The best fit for this model is shown in the panel b of Fig. 3: the residuals are of course largely reduced with respect to the other fit and the general behaviour is much better described, but smaller amplitude systematic deviations remain apparent.

To quantify the timing noise we can calculate the Δ_8 parameter defined by Arzoumanian et al. (1994) as:

$$\Delta_8 = \log(10^{24}|\dot{\nu}|/6\nu). \quad (3)$$

For PSR 0540–69 instead of the measured $\ddot{\nu}$, whose large value is related to the regular spin down rather than the timing noise,

we used the correction that takes into account the residuals shown in Fig. 3a. A reliable estimate of this correction is given by the difference between the third degree coefficient of the best fit parameters of the sixth and third degree polynomials. This difference was found equal to $2.27 \times 10^{-22} \text{ Hz s}^{-2}$ and gives $\Delta_8 = 0.28$, higher than all the values of the sample of Arzoumanian et al. (1994). Note that PSR B0540-69 lies well in the upper part of the plot Δ_8 vs. \dot{P} given by these authors.

To compare our results with those of Zhang et al. (2001) we divided our data into two subsets, before and after the time of the glitch, assumed at MJD 51325 – the interval of possible epochs given by Zhang et al. (2001), spans 45 days – and applied a cubic polynomial fit to each subset. We obtained acceptable fits, characterized by nearly zero residuals; resulting best fit values for the two intervals are reported in Table 2, the ephemerides are given in Table 3. Propagating the parameters of Table 3 to the epoch of the glitch we obtained a marginal detection for the frequency change $\Delta\nu/\nu = (1.8 \pm 1.0) \times 10^{-9}$, whereas more significant differences were found for the first and second derivative: $\Delta\dot{\nu}/\dot{\nu} = (1.69 \pm 0.01) \times 10^{-4}$ and $\Delta\ddot{\nu}/\ddot{\nu} = (2.043 \pm 0.001) \times 10^{-3}$. The significance of these parameters' differences can be largely affected by the timing noise systematics. To verify this hypothesis we performed a similar analysis on other data subsets selected by changing the separation epochs and values of $\Delta\nu/\nu$ of the same order and similar significance were found. This last finding addressed us to interpret the marginal detection of frequency jump at the glitch epoch claimed by Zhang et al. (2001) as a not genuine result but due to the pulse phase analysis in presence of strong timing noise.

3.3. The braking index

As discussed in the Introduction, a relevant difference between our previous results (Mineo et al. 1999) and those of Zhang et al. (2001) is in the value of the braking index: we essentially confirmed the estimates of Deeter et al. (1998), Hirayama et al. (2002), while Zhang et al. (2001) gave the value of 1.81, about 14% smaller, but significantly different when considering the associated uncertainties. Using the new ephemerides given in Table 3, we computed for the two intervals the values of n and obtained 2.1272 ± 0.0003 and 2.122 ± 0.001 for the first and second interval, respectively.

A change in the timing parameters implies a variation of the braking index:

$$\frac{\Delta n}{n} = \frac{\Delta\nu}{\nu} - 2\frac{\Delta\dot{\nu}}{\dot{\nu}} + \frac{\Delta\ddot{\nu}}{\ddot{\nu}}. \quad (4)$$

From the above results it is clear that the parameter responsible for the much lower value of n measured by Zhang et al. (2001) is the second frequency derivative, for which these authors reported the value of $(3.23 \pm 0.12) \times 10^{-21} \text{ s}^{-2}$, just 15% smaller than our result.

This discrepancy is likely due to the presence of such high timing noise, because the data set considered by Zhang et al. (2001) spans a rather narrow time interval with respect to that considered by us. To further investigate this point we computed the braking index in several independent time intervals, evaluating the best corrections to the pulsar ephemerides in each

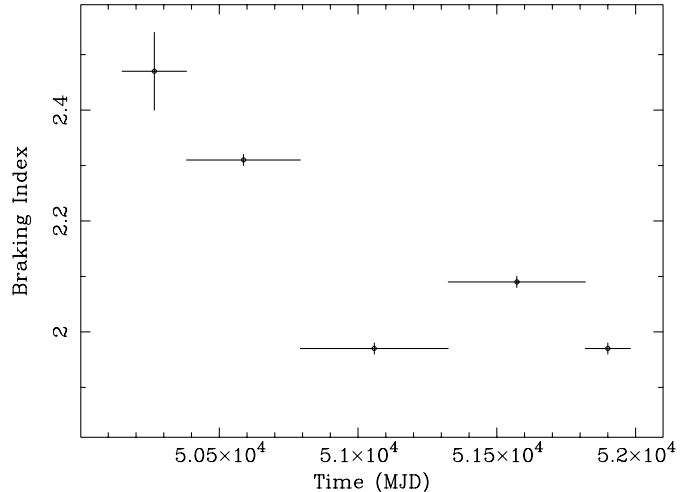


Fig. 4. The values of the braking index computed in several intervals plotted as a function of the central time of the interval. These large changes are a consequence of the timing noise affecting the second derivative of the pulsar frequency.

of them. The resulting values are shown in Fig. 4: they range from 1.97 to 2.47. Again the largest variation is due to the estimates of second derivative of the pulsar frequency, which differs by $\sim 20\%$ between the various intervals. We conclude that reliable estimates of the braking index can be obtained only considering the longest time intervals in which a good fit of phases (or TOA) with Eq. (2) can be obtained, likely spanning several years. The use of shorter intervals can introduce a bias due to the timing noise.

4. Discussion

The only way to study the timing noise of PSR B0540–69 is the use of a dense set of X-ray observations, like that of RXTE, because this young pulsar is in the Large Magellanic Cloud and its flux is too weak to be monitored in the radio band. Our analysis on a large database of X-ray observations of PSR B0540–69, covering more than 5 years, provided good evidence for a relevant timing noise affecting the phase of the pulsed signal. In particular, we showed that the best fit of a third degree polynomial, including up to the second frequency derivative, gives phase residuals up to a few cycles and that residuals as large as 0.4 remain even when a sixth degree polynomial is used. Assuming that the difference in the second derivative obtained from these best fits is a measure of its fluctuations, we evaluated the Δ_8 parameter (Arzoumanian et al. 1994) which was found equal to 0.28, confirming the high level of timing noise. Taking into account that even larger variations of this derivative are also found when polynomial best fits are performed over shorter time intervals, this result could be considered a lower limit. Furthermore, it supports the finding that timing noise is stronger in young pulsars with a high \dot{P} .

A consequence of this high timing noise is that the glitch claimed by Zhang et al. (2001) cannot be confirmed. The frequency difference of this event given by these authors is very small, about $0.04 \mu\text{Hz}$. The glitch cannot be detected directly as a sudden frequency jump because it is less than the

Table 2. Corrections to the timing parameters of PSR B0540–69.

| Time Interval | $\Delta\nu$ (Hz) | $\Delta\dot{\nu}$ (Hz s ⁻¹) | $\Delta\ddot{\nu}$ (Hz s ⁻²) |
|---------------------|---------------------------|--|---|
| (1) $t < 51325$ MJD | $-1.359(2)\times 10^{-7}$ | $1.68(2)\times 10^{-15}$ | $8.00(4)\times 10^{-23}$ |
| (2) $t > 51325$ MJD | $2.487(9)\times 10^{-6}$ | $-2.94(2)\times 10^{-14}$ | $7.2(2)\times 10^{-23}$ |

Table 3. Frequency ephemerides obtained from a phase coherent analysis before and after MJD 51325.

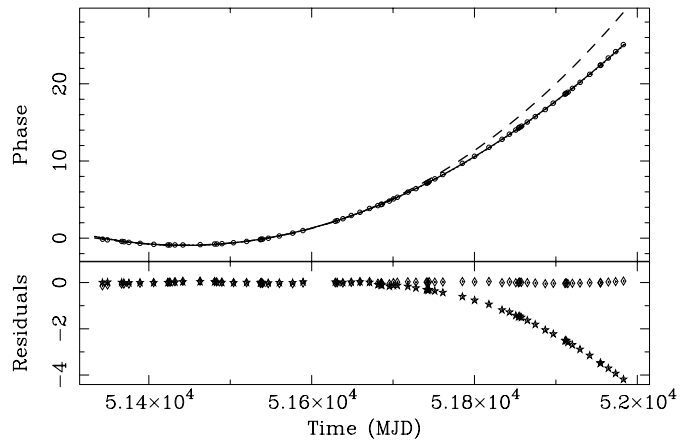
| Time Interval | t_0 (MJD) | ν (Hz) | $\dot{\nu}$ ($\times 10^{-10}$ Hz s ⁻¹) | $\ddot{\nu}$ ($\times 10^{-21}$ Hz s ⁻²) | n |
|---------------------|------------------|------------------|---|--|-----------|
| (1) $t < 51325$ MJD | 50372.5481748585 | 19.8158310541(2) | -1.8807101(2) | 3.7970(4) | 2.1272(3) |
| (2) $t > 51325$ MJD | 50372.5481748585 | 19.815833677(9) | -1.881021(2) | 3.789(2) | 2.122(1) |

uncertainties in the frequency measurements which are typically of the order of a few μHz , and in the best conditions of a few tenth of μHz . Zhang et al. (2001) also excluded that this effect can be due to timing noise, but their conclusion is affected by the use of a shorter time interval that does not allow an accurate analysis of the timing noise.

Our results show that frequency differences of the same order of that given by Zhang et al. (2001) are usually found when different selections of time intervals are considered and they do not depend upon a well-defined episode.

From the timing noise analysis we were also able to show how much the first and second derivatives of the pulsar frequency are stable in time. We found that the former can have fluctuations of amplitude of about 10^{-4} , while for the latter fluctuations can be much higher, and in some cases the estimates can differ by ~ 10 – 20% , depending on the length of the time interval taken into account. Such large variations affect the evaluation of the braking index, particularly when it is found by the fitting of Eq. (2) to the pulse phases. We showed that when the longest possible intervals are considered, n turns out to be very close to 2.12, in agreement with several previous estimates, while values like that given by Zhang et al. (2001) are obtained over shorter intervals. We verified this interpretation by fitting Eq. (2) to the same subset of RXTE observations used by these authors (more specifically, the fit was performed on RXTE observations from row 82 to row 114 of Table A1) and derived from the best fit ephemeris $n = 1.854 \pm 0.003$. However, when these parameters are used to extrapolate the phase shift to the entire subset of data after the epoch of the glitch claimed by Zhang et al. (2001), they produce a systematic deviation of the residuals which increases with the elapsed time, as shown in Fig. 5.

Finally, we note that the agreement of our estimate of the braking index with those derived from ASCA (Hirayama et al. 2002) and BeppoSAX (Mineo et al. 1999) data can be easily understood on the basis of the rather long time intervals covered by the observations. They are too sparse to provide good information on the timing noise but can give an accurate evaluation of the mean second derivative.

**Fig. 5.** Phase residuals obtained extrapolating the ephemerides solution of Zhang et al. (2001) to the entire subset of data after the epoch MJD 51325.

Acknowledgements. The authors are very grateful to the referee, R. N. Manchester, for the relevant comments and suggestions that greatly improved the scientific content of the paper. This work has been partially supported by the Italian Space Agency (ASI).

Appendix

The log of the observations and the corresponding TOAs and frequencies are given in Table A1 available in electronic form at CDS via anonymous ftp to [cdsarc.u-strasbg.fr](ftp://cdsarc.u-strasbg.fr) (130.79.128.5) or via

<http://cdsweb.u-strasbg.fr/cgi-bin/qcat?J/A+A/402/647>.

The content of the data columns is: central epoch of the observation (Col. 2), total duration (Col. 3), exposure time (Col. 4), TOA and error (Cols. 5 and 6; only for RXTE observations) and frequency with the relative error (Cols. 6 and 7) for each observation analyzed.

References

- Arzoumanian, Z., Nice, D. J., Taylor, J. H., & Thorsett, S. E. 1994, *ApJ*, 422, 671
Boella, G., Butler, R. C., Perola, G. C., et al. 1997a, *A&AS*, 122, 299

- Boella, G., Chiappetti, L., Conti, G., et al. 1997b, *A&AS*, 122, 327
- Boyd, P. T., van Citters, G. W., Dolan, J. F., et al. 1995, *ApJ*, 448, 365
- Caraveo, P. A., Bignami, G. F., Mereghetti, S., & Mombelli, M. 1992, *ApJ*, 395, L103
- Deeter, J. E., Nagase, F., & Boyton, P. E. 1999, *ApJ*, 512, 300
- Hirayama, M., Nagase, F., Gunji, S., Sekimoto, Y., & Saito, Y. 1996, *ASCA News*, Issue 4, 18
- Hirayama, M., Nagase, F., Endo, T., Kawai, N., & Itoh, M. 2002, *MNRAS*, 333, 603
- Kaaret, P., Marshall, H. L., Aldcroft, T. L., et al. 2001, *ApJ*, 546, 1159
- Lyne, A. 1999, in *Proc. of the Colloq., Amsterdam Pulsar Timing, General Relativity and the Internal Structure of Neutron Stars*, 24–27 September 1996
- Makishima, K., Tashiro, M., Ebisawa, K., et al. 1996, *PASJ*, 48, 171
- Manchester, R. N., & Peterson, B. A. 1989, *ApJ*, 342, L23
- Manchester, R. N., Mar, D. P., Lyne, A. G., Kaspi, V. M., & Johnston, S. 1993, *ApJ*, 403, L29
- Middleditch, J., & Pennypacker, C. R. 1985, *Nature*, 313, 659
- Mineo, T., Cusumano, G., Massaro, E., et al. 1999, *A&A*, 348, 519
- Nagase, F., Deeter, J., Lewis, W., et al. 1990, *ApJ*, 351, L13
- Ögelman, H., & Hasinger, G. 1990, *ApJ*, 353, L21
- Ohashi, T., Ebisawa, K., Fukazawa, Y., et al. 1996, *PASJ*, 48, 1570
- Seward, F. D., Harnden, F. R., & Helfand, D. J. 1984, *ApJ*, 287, L19
- Standish, E. M. 1982, *A&A*, 114, 297
- Tanaka, Y., Inoue, H., & Holt, S. S. 1994, *PASJ*, 46, L37
- Wong, T., Backer, D. C., & Lyne, A. G. 2001, *ApJ*, 548, 447
- Zhang, W., Marshall, F. E., Gotthelf, E. V., et al. 2001, *ApJ*, 554, 177